# Contents

# List of Figures

# List of Tables

# Chapter 14

# Two-Dimensional Phase Flows

We've seen how, for one-dimensional dynamical systems $\dot{u} = f(u)$, the possibilities in terms of the behavior of the system are in fact quite limited. Starting from an arbitrary initial condition $u(0)$, the phase flow is monotonically toward the first stable fixed point encountered. (That point may lie at infinity.) No oscillations are possible[1]. For $N = 2$ phase flows, a richer set of possibilities arises, as we shall now see.

## 14.1 Harmonic Oscillator and Pendulum

### 14.1.1 Simple harmonic oscillator

A one-dimensional harmonic oscillator obeys the equation of motion,

$$m\frac{d^2x}{dt^2} = -kx \quad , \tag{14.1}$$

where $m$ is the mass and $k$ the force constant (of a spring). If we define $v = \dot{x}$, this may be written as the $N = 2$ system,

$$\frac{d}{dt}\begin{pmatrix} x \\ v \end{pmatrix} = \begin{pmatrix} 0 & 1 \\ -\Omega^2 & 0 \end{pmatrix}\begin{pmatrix} x \\ v \end{pmatrix} = \begin{pmatrix} v \\ -\Omega^2\, x \end{pmatrix} \quad , \tag{14.2}$$

where $\Omega = \sqrt{k/m}$ has the dimensions of frequency (inverse time). The solution is well known:

$$\begin{aligned} x(t) &= x_0\, \cos(\Omega t) + \frac{v_0}{\Omega}\, \sin(\Omega t) \\ v(t) &= v_0\, \cos(\Omega t) - \Omega\, x_0\, \sin(\Omega t) \quad . \end{aligned} \tag{14.3}$$

The phase curves are ellipses:

$$\Omega\, x^2(t) + \Omega^{-1}\, v^2(t) = C \quad , \tag{14.4}$$

[1] If phase space itself is multiply connected, *e.g.* a circle, then the system can oscillate by moving around the circle.

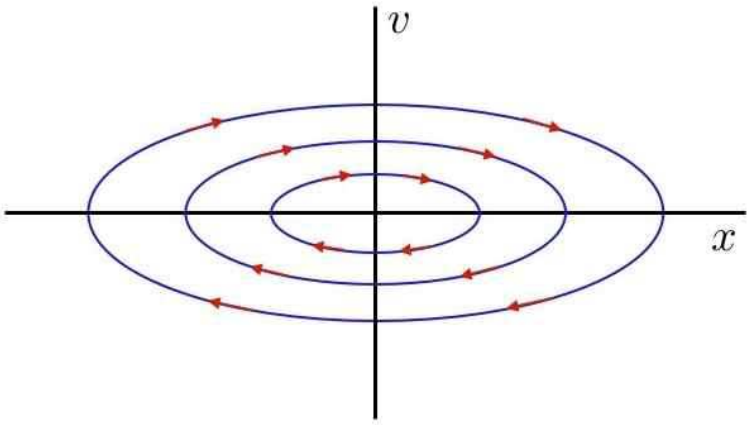


Figure 14.1: Phase curves for the harmonic oscillator.

where the constant $C = \Omega\, x_0^2 + \Omega^{-1}\, v_0^2$. A sketch of the phase curves and of the phase flow is shown in Fig. 14.1. Note that the $x$ and $v$ axes have different dimensions. Note also that the origin is a fixed point, however, unlike the $N = 1$ systems studied in the first lecture, here the phase flow can avoid the fixed points, and oscillations can occur.

Incidentally, eqn. 14.2 is linear, and may be solved by the following method. Write the equation as $\dot{\boldsymbol{\varphi}} = M\boldsymbol{\varphi}$, with

$$\boldsymbol{\varphi} = \begin{pmatrix} x \\ \dot{x} \end{pmatrix} \qquad \text{and} \qquad M = \begin{pmatrix} 0 & 1 \\ -\Omega^2 & 0 \end{pmatrix} \tag{14.5}$$

The formal solution to $\dot{\boldsymbol{\varphi}} = M\boldsymbol{\varphi}$ is

$$\boldsymbol{\varphi}(t) = e^{Mt}\, \boldsymbol{\varphi}(0) \quad . \tag{14.6}$$

What do we mean by the exponential of a matrix? We mean its Taylor series expansion:

$$e^{Mt} = \mathbb{I} + Mt + \tfrac{1}{2!}\, M^2\, t^2 + \tfrac{1}{3!}\, M^3\, t^3 + \ldots \quad . \tag{14.7}$$

Note that

$$\begin{aligned} M^2 &= \begin{pmatrix} 0 & 1 \\ -\Omega^2 & 0 \end{pmatrix} \begin{pmatrix} 0 & 1 \\ -\Omega^2 & 0 \end{pmatrix} \\ &= \begin{pmatrix} -\Omega^2 & 0 \\ 0 & -\Omega^2 \end{pmatrix} = -\Omega^2\, \mathbb{I} \quad , \end{aligned} \tag{14.8}$$

hence

$$M^{2k} = (-\Omega^2)^k\, \mathbb{I} \qquad , \qquad M^{2k+1} = (-\Omega^2)^k\, M \quad . \tag{14.9}$$

Thus,

$$\begin{aligned} e^{Mt} &= \sum_{k=0}^{\infty} \frac{1}{(2k)!} (-\Omega^2 t^2)^k \cdot \mathbb{I} + \sum_{k=0}^{\infty} \frac{1}{(2k+1)!} (-\Omega^2 t^2)^k \cdot Mt \\ &= \cos(\Omega t) \cdot \mathbb{I} + \Omega^{-1} \sin(\Omega t) \cdot M \\ &= \begin{pmatrix} \cos(\Omega t) & \Omega^{-1} \sin(\Omega t) \\ -\Omega \, \sin(\Omega t) & \cos(\Omega t) \end{pmatrix} \quad . \end{aligned} \tag{14.10}$$

Plugging this into eqn. 14.6, we obtain the desired solution.

For the damped harmonic oscillator, we have

$$\ddot{x} + 2\beta\dot{x} + \Omega^2 x = 0 \qquad \Longrightarrow \qquad M = \begin{pmatrix} 0 & 1 \\ -\Omega^2 & -2\beta \end{pmatrix} \quad . \tag{14.11}$$

The phase curves then spiral inward to the fixed point at $(0, 0)$.

### 14.1.2 Pendulum

Next, consider the simple pendulum, composed of a mass point $m$ affixed to a massless rigid rod of length $\ell$.

$$m\ell^2 \, \ddot{\theta} = -mg\ell \sin\theta \quad . \tag{14.12}$$

This is equivalent to

$$\frac{d}{dt} \begin{pmatrix} \theta \\ \omega \end{pmatrix} = \begin{pmatrix} \omega \\ -\Omega^2 \, \sin\theta \end{pmatrix} \quad , \tag{14.13}$$

where $\omega = \dot{\theta}$ is the angular velocity, and where $\Omega = \sqrt{g/\ell}$ is the natural frequency of small oscillations.

The phase curves for the pendulum are shown in Fig. 14.2. The small oscillations of the pendulum are essentially the same as those of a harmonic oscillator. Indeed, within the small angle approximation, $\sin\theta \approx \theta$, and the pendulum equations of motion are exactly those of the harmonic oscillator. These oscillations are called *librations*. They involve a back-and-forth motion in real space, and the phase space motion is contractable to a point, in the topological sense. However, if the initial angular velocity is large enough, a qualitatively different kind of motion is observed, whose phase curves are *rotations*. In this case, the pendulum bob keeps swinging around in the same direction, because, as we'll see in a later lecture, the total energy is sufficiently large. The phase curve which separates these two topologically distinct motions is called a *separatrix*.

## 14.2 General $N = 2$ Systems

The general form to be studied is

$$\frac{d}{dt} \begin{pmatrix} x \\ y \end{pmatrix} = \begin{pmatrix} V_x(x, y) \\ V_y(x, y) \end{pmatrix} \quad . \tag{14.14}$$

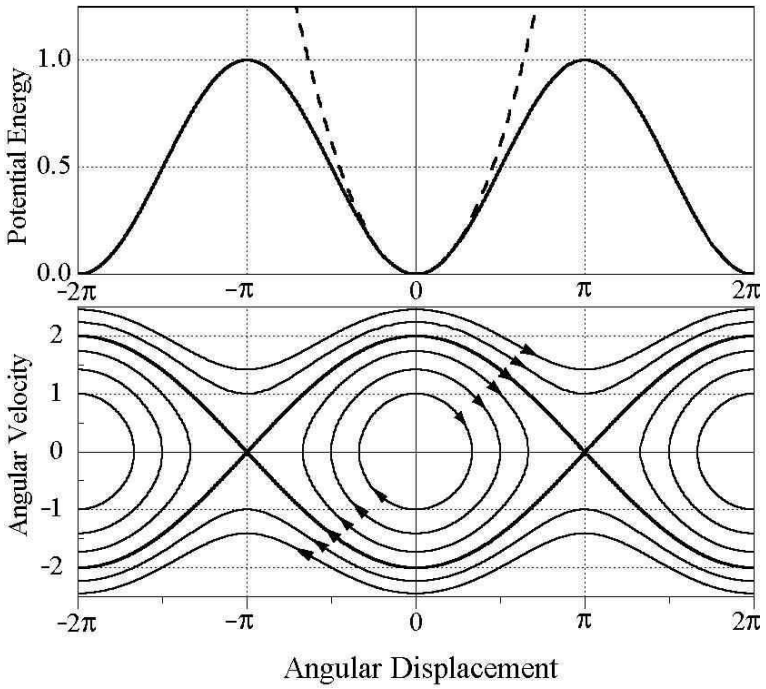


Figure 14.2: Phase curves for the simple pendulum. The *separatrix* divides phase space into regions of vibration and libration.

Special cases include autonomous second order ODEs, *viz.*

$$\ddot{x} = f(x, \dot{x}) \qquad \Longrightarrow \qquad \frac{d}{dt}\begin{pmatrix} x \\ v \end{pmatrix} = \begin{pmatrix} v \\ f(x,v) \end{pmatrix} \quad , \tag{14.15}$$

of the type which occur in one-dimensional mechanics.

### 14.2.1 The damped driven pendulum

Another example is that of the damped and driven harmonic oscillator,

$$\frac{d^2\phi}{ds^2} + \gamma \frac{d\phi}{ds} + \sin\phi = j \quad . \tag{14.16}$$

This is equivalent to a model of a resistively and capacitively shunted Josephson junction, depicted in fig. 14.3. If $\phi$ is the superconducting phase difference across the junction, the current through the junction is given by $I_J = I_{\rm c} \sin\phi$, where $I_{\rm c}$ is the *critical current*. The current carried by the resistor is $I_R = V/R$ from Ohm's law, and the current from the capacitor is $I_C = \dot{Q}$. Finally, the *Josephson relation* relates the voltage $V$ across the junction to the superconducting phase difference $\phi$: $V = (\hbar/2e)\,\dot{\phi}$. Summing up the parallel currents, we have that the total current $I$ is given by

$$I = \frac{\hbar C}{2e}\,\ddot{\phi} + \frac{\hbar}{2eR}\,\dot{\phi} + I_{\rm c}\,\sin\phi \quad , \tag{14.17}$$

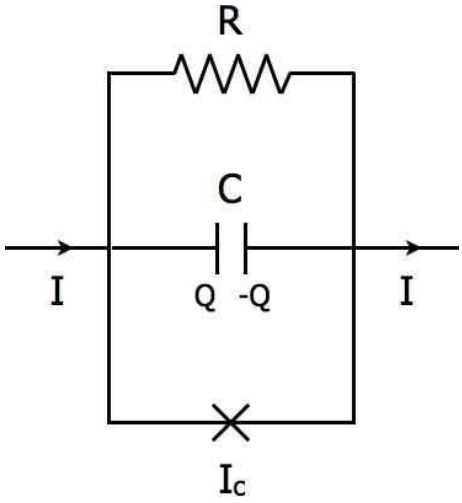


Figure 14.3: . The resistively and capacitively shunted Josephson junction. The Josephson junction is the X element at the bottom of the figure.

which, again, is equivalent to a damped, driven pendulum.

This system also has a mechanical analog. Define the 'potential'

$$U(\phi) = -I_{\rm c}\,\cos\phi - I\phi \quad . \tag{14.18}$$

The equation of motion is then

$$\frac{\hbar C}{2e}\,\ddot{\phi} + \frac{\hbar}{2eR}\,\dot{\phi} = -\frac{\partial U}{\partial \phi} \quad . \tag{14.19}$$

Thus, the combination $\hbar C/2e$ plays the role of the inertial term (mass, or moment of inertia), while the combination $\hbar/2eR$ plays the role of a damping coefficient. The potential $U(\phi)$ is known as the *tilted washboard potential*, for obvious reasons. (Though many of you have perhaps never seen a washboard.)

The model is adimensionalized by defining the Josephson plasma frequency $\omega_{\rm p}$ and the $RC$ time constant $\tau$:

$$\omega_{\rm p} \equiv \sqrt{\frac{2eI_{\rm c}}{\hbar C}} \qquad , \qquad \tau \equiv RC \quad . \tag{14.20}$$

The dimensionless combination $\omega_{\rm p}\tau$ then enters the adimensionalized equation as the sole control parameter:

$$\frac{I}{I_{\rm c}} = \frac{d^2\phi}{ds^2} + \frac{1}{\omega_{\rm p}\tau}\,\frac{d\phi}{ds} + \sin\phi \quad , \tag{14.21}$$

where $s = \omega_{\rm p} t$. In the Josephson junction literature, the quantity $\beta \equiv 2eI_{\rm c}R^2C/\hbar = (\omega_{\rm p}\tau)^2$, known as the *McCumber-Stewart* parameter, is a dimensionless measure of the damping (large $\beta$ means small damping). In terms of eqn. 14.16, we have $\gamma = (\omega_{\rm p}\tau)^{-1}$ and $j = I/I_{\rm c}$.

We can write the second order ODE of eqn. 14.16 as two coupled first order ODEs:

$$\frac{d}{dt}\begin{pmatrix}\phi\\ \omega\end{pmatrix} = \begin{pmatrix}\omega\\ j - \sin\phi - \gamma\,\omega\end{pmatrix} \quad , \tag{14.22}$$

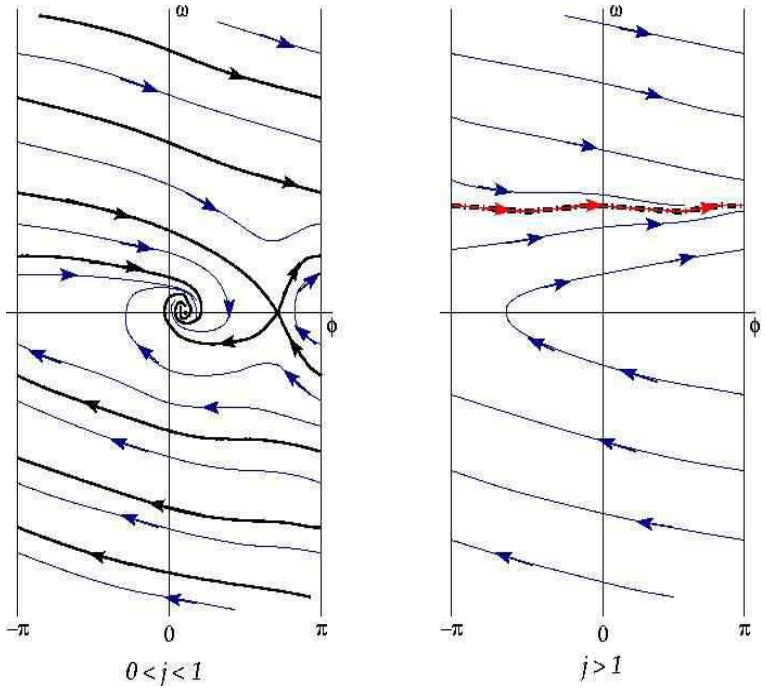


Figure 14.4: Phase flows for the equation $\ddot{\phi} + \gamma^{-1}\dot{\phi} + \sin\phi = j$. Left panel: $0 < j < 1$; note the separatrix (in black), which flows into the stable and unstable fixed points. Right panel: $j > 1$. The red curve overlying the thick black dot-dash curve is a *limit cycle*.

where $\omega = \dot{\phi}$. Phase space is a cylinder, $\mathbb{S}^1 \times \mathbb{R}^1$.

The quantity $\omega_{\rm p}\tau$ typically ranges from $10^{-3}$ to $10^3$ in Josephson junction applications. If $\omega_{\rm p}\tau$ is small, then the system is heavily damped, and the inertial term $d^2\phi/ds^2$ can be neglected. One then obtains the $N = 1$ system

$$\gamma\,\frac{d\phi}{ds} = j - \sin\phi \quad . \tag{14.23}$$

If $|j| < 1$, then $\phi(s)$ evolves to the first stable fixed point encountered, where $\phi^* = \sin^{-1}(j)$ and $\cos\phi^* = \sqrt{1-j^2}$. Since $\phi(s) \to \phi^*$ is asymptotically a constant, the voltage drop $V$ must then vanish, as a consequence of the Josephson relation $V = (\hbar/2e)\,\dot{\phi}$. This, there is current flowing with no voltage drop!

If $|j| > 1$, the RHS never vanishes, in which case $\phi(s)$ is monotonic. We then can integrate the differential equation

$$dt = \frac{\hbar}{2eR}\cdot\frac{d\phi}{I - I_{\rm c}\,\sin\phi} \quad . \tag{14.24}$$

Asymptotically the motion is periodic, with the period $T$ obtained by integrating over the interval $\phi \in [0, 2\pi]$. One finds

$$T = \frac{\hbar}{2eR}\cdot\frac{2\pi}{\sqrt{I^2 - I_{\rm c}^2}} \quad . \tag{14.25}$$

The time-averaged voltage drop is then

$$\langle V \rangle = \frac{\hbar}{2e} \langle \dot{\phi} \rangle = \frac{\hbar}{2e} \cdot \frac{2\pi}{T} = R\sqrt{I^2 - I_{\rm c}^2} \quad . \tag{14.26}$$

This is the physics of the *current-biased resistively and capacitively shunted Josephson junction* in the strong damping limit. It is 'current-biased' because we are specifying the current $I$. Note that Ohm's law is recovered at large values of $I$.

For general $\omega_{\rm p}\tau$, we can still say quite a bit. At a fixed point, both components of the vector field $\boldsymbol{V}(\phi, \omega)$ must vanish. This requires $\omega = 0$ and $j = \sin\phi$. Therefore, there are two fixed points for $|j| < 1$, one a saddle point and the other a stable spiral. For $|j| > 1$ there are no fixed points, and asymptotically the function $\phi(t)$ tends to a periodic *limit cycle* $\phi_{\rm LC}(t)$. The flow is sketched for two representative values of $j$ in Fig. 14.4.

### 14.2.2 Classification of $N = 2$ fixed points

Suppose we have solved the fixed point equations $V_x(x^*, y^*) = 0$ and $V_y(x^*, y^*) = 0$. Let us now expand about the fixed point, writing

$$\begin{aligned} \dot{x} &= \left.\frac{\partial V_x}{\partial x}\right|_{(x^*,y^*)} (x - x^*) + \left.\frac{\partial V_x}{\partial y}\right|_{(x^*,y^*)} (y - y^*) + \dots \\ \dot{y} &= \left.\frac{\partial V_y}{\partial x}\right|_{(x^*,y^*)} (x - x^*) + \left.\frac{\partial V_y}{\partial y}\right|_{(x^*,y^*)} (y - y^*) + \dots \quad . \end{aligned} \tag{14.27}$$

We define

$$u_1 = x - x^* \qquad , \qquad u_2 = y - y^* \quad , \tag{14.28}$$

which, to linear order, satisfy

$$\frac{d}{dt}\begin{pmatrix} u_1 \\ \\ u_2 \end{pmatrix} = \overbrace{\begin{pmatrix} a & b \\ \\ c & d \end{pmatrix}}^{M} \begin{pmatrix} u_1 \\ \\ u_2 \end{pmatrix} + \mathcal{O}(u^2) \quad . \tag{14.29}$$

The formal solution to $\dot{\boldsymbol{u}} = M\boldsymbol{u}$ is

$$\boldsymbol{u}(t) = \exp(Mt)\,\boldsymbol{u}(0) \quad , \tag{14.30}$$

where $\exp(Mt) = \sum_{n=0}^{\infty} \frac{1}{n!} (Mt)^n$ is the exponential of the matrix $Mt$.

The behavior of the system is determined by the eigenvalues of $M$, which are roots of the characteristic equation $P(\lambda) = 0$, where

$$\begin{aligned} P(\lambda) &= \det(\lambda \mathbb{I} - M) \\ &= \lambda^2 - T\lambda + D \quad , \end{aligned} \tag{14.31}$$

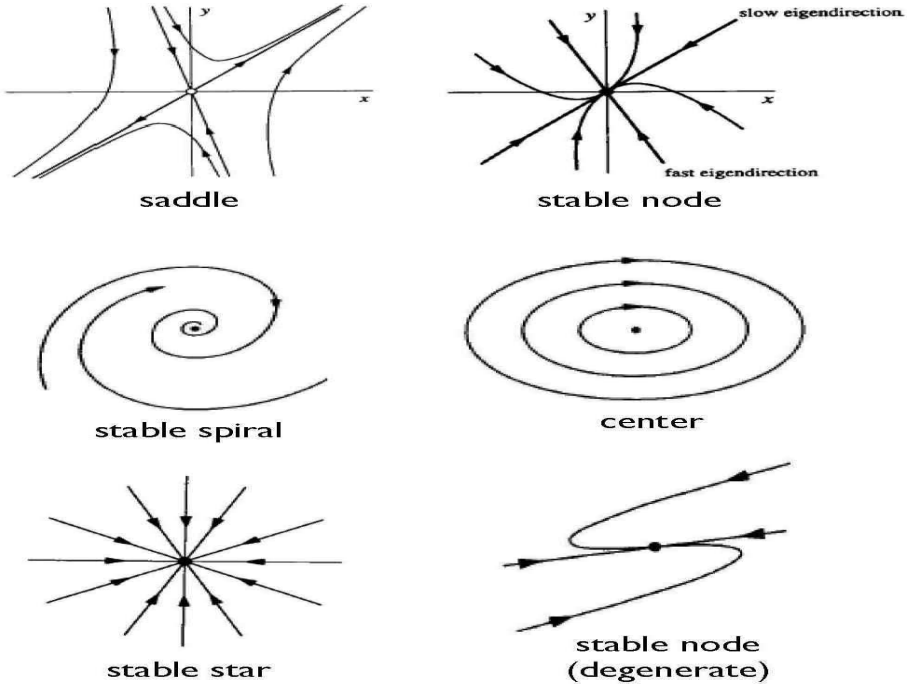


Figure 14.5: Fixed point zoo for $N = 2$ systems. Not shown: unstable versions of node, spiral, and star (reverse direction of arrows to turn stable into unstable).

with $T = a + d = \mathrm{Tr}(M)$ and $D = ad - bc = \det(M)$. The two eigenvalues are therefore

$$\lambda_\pm = \tfrac{1}{2}\Big(T \pm \sqrt{T^2 - 4D}\Big) \quad . \tag{14.32}$$

To see why the eigenvalues control the behavior, let us expand $\boldsymbol{u}(0)$ in terms of the eigenvectors of $M$. Since $M$ is not necessarily symmetric, we should emphasize that we expand $\boldsymbol{u}(0)$ in terms of the *right* eigenvectors of $M$, which satisfy

$$M\boldsymbol{\psi}_a = \lambda_a \boldsymbol{\psi}_a \quad , \tag{14.33}$$

where the label $a$ runs over the symbols $+$ and $-$, as in (14.32). We write

$$\boldsymbol{u}(t) = \sum_a C_a(t)\,\boldsymbol{\psi}_a \quad . \tag{14.34}$$

Since (we assume) the eigenvectors are *linearly independent*, the equation $\dot{\boldsymbol{u}} = M\boldsymbol{u}$ becomes

$$\dot{C}_a = \lambda_a\, C_a \quad , \tag{14.35}$$

with solution

$$C_a(t) = e^{\lambda_a t}\, C_a(0) \quad . \tag{14.36}$$

Thus, the coefficients of the eigenvectors $\boldsymbol{\psi}_a$ will *grow* in magnitude if $|\lambda_a| > 1$, and will *shrink* if $|\lambda_a| < 1$.

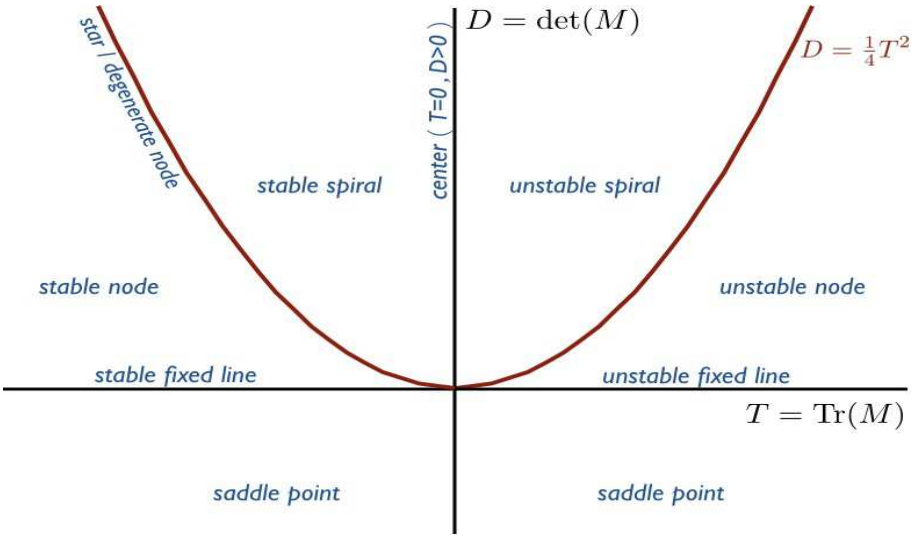


Figure 14.6: Complete classification of fixed points for the $N = 2$ system.

### 14.2.3 The fixed point zoo

- **Saddles** : When $D < 0$, both eigenvalues are real; one is positive and one is negative, *i.e.* $\lambda_+ > 0$ and $\lambda_- < 0$. The right eigenvector $\boldsymbol{\psi}_-$ is thus the *stable direction* while $\boldsymbol{\psi}_+$ is the *unstable direction*.

- **Nodes** : When $0 < D < \frac{1}{4}T^2$, both eigenvalues are real and of the same sign. Thus, both right eigenvectors correspond to stable or to unstable directions, depending on whether $T < 0$ (stable; $\lambda_- < \lambda_+ < 0$) or $T < 0$ (unstable; $\lambda_+ > \lambda_- > 0$). If $\lambda_\pm$ are distinct, one can distinguish *fast* and *slow* eigendirections, based on the magnitude of the eigenvalues.

- **Spirals** : When $D > \frac{1}{4}T^2$, the discriminant $T^2 - 4D$ is negative, and the eigenvalues come in a complex conjugate pair: $\lambda_- = \lambda_+^*$. The real parts are given by $\mathrm{Re}(\lambda_\pm) = \frac{1}{2}T$, so the motion is stable (*i.e.* collapsing to the fixed point) if $T < 0$ and unstable (*i.e.* diverging from the fixed point) if $T > 0$. The motion is easily shown to correspond to a spiral. One can check that the spiral rotates counterclockwise for $a > d$ and clockwise for $a < d$.

- **Degenerate Cases** : When $T = 0$ we have $\lambda_\pm = \pm\sqrt{-D}$. For $D < 0$ we have a saddle, but for $D > 0$ both eigenvalues are imaginary: $\lambda_\pm = \pm i\sqrt{D}$. The orbits do not collapse to a point, nor do they diverge to infinity, in the $t \to \infty$ limit, as they do in the case of the stable and unstable spiral. The fixed point is called a *center*, and it is surrounded by closed trajectories.

  When $D = \frac{1}{4}T^2$, the discriminant vanishes and the eigenvalues are degenerate. If the rank of $M$ is two, the fixed point is a stable ($T < 0$) or unstable ($T > 0$) *star*. If $M$ is degenerate and of rank one, the fixed point is a *degenerate node*.

  When $D = 0$, one of the eigenvalues vanishes. This indicates a *fixed line* in phase space, since any point on that line will not move. The fixed line can be stable or unstable, depending on whether the remaining eigenvalue is negative (stable, $T < 0$), or positive (unstable, $T > 0$).

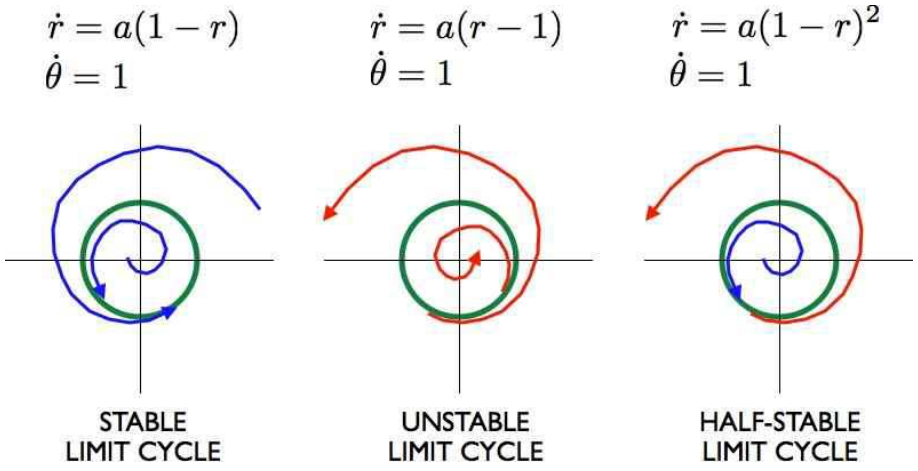


Figure 14.7: Stable, unstable, and half-stable limit cycles.

Putting it all together, an example of a phase portrait is shown in Fig. 14.8. Note the presence of an *isolated, closed trajectory*, which is called a *limit cycle*. Many self-sustained physical oscillations, *i.e.* oscillations with no external forcing, exhibit limit cycle behavior. Limit cycles, like fixed points, can be stable or unstable, or partially stable. Limit cycles are inherently nonlinear. While the linear equation $\dot{\boldsymbol{\varphi}} = M\,\boldsymbol{\varphi}$ can have periodic solutions if $M$ has purely imaginary eigenvalues, these periodic trajectories are not *isolated*, because $\lambda\,\boldsymbol{\varphi}(t)$ is also a solution. The amplitude of these linear oscillations is fixed by the initial conditions, whereas for limit cycles, the amplitude is inherent from the dynamics itself, and the initial conditions are irrelevant (for a stable limit cycle).

In fig. 14.7 we show simple examples of stable, unstable, and half-stable limit cycles. As we shall see when we study nonlinear oscillations, the Van der Pol oscillator,

$$\ddot{x} + \mu(x^2 - 1)\,\dot{x} + x = 0 \quad , \tag{14.37}$$

with $\mu > 0$ has a stable limit cycle. The physics is easy to apprehend. The coefficient of the $\dot{x}$ term in the equation of motion is positive for $|x| > 1$ and negative for $|x| < 1$. Interpreting this as a coefficient of friction, we see that the friction is positive, *i.e.* dissipating energy, when $|x| > 1$ but *negative*, *i.e.* accumulating energy, for $|x| < 1$. Thus, any small motion with $|x| < 1$ is *amplified* due to the negative friction, and would increase without bound were it not for the fact that the friction term reverses its sign and becomes dissipative for $|x| > 1$. The limit cycle for $\mu \gg 1$ is shown in fig. 14.9.

### 14.2.4 Fixed points for $N = 3$ systems

For an $N = 2$ system, there are five generic types of fixed points. They are classified according to the eigenvalues of the linearized dynamics at the fixed point. For a real $2 \times 2$ matrix, the eigenvalues must

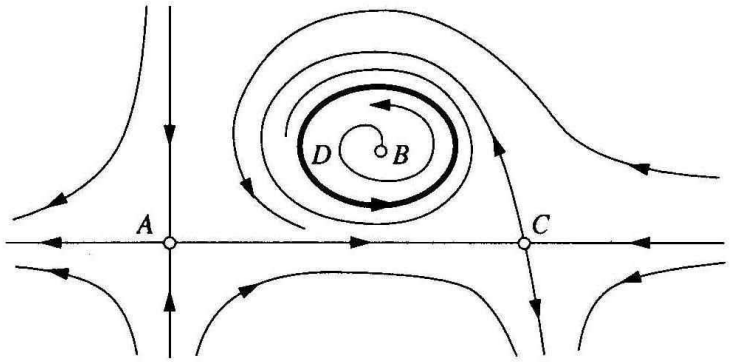


Figure 14.8: Phase portrait for an $N = 2$ flow including saddles (A,C), unstable spiral (B), and limit cycle (D).

be real or else must be a complex conjugate pair. The five types of fixed points are then

$$\begin{aligned}
\lambda_1 > 0 \quad , \ \lambda_2 > 0 \quad &: \quad \text{(1) unstable node} \\
\lambda_1 > 0 \quad , \ \lambda_2 < 0 \quad &: \quad \text{(2) saddle point} \\
\lambda_1 < 0 \quad , \ \lambda_2 < 0 \quad &: \quad \text{(3) stable node} \\
\mathsf{Re}\,\lambda_1 > 0 \quad , \ \lambda_2 = \lambda_1^* \quad &: \quad \text{(4) unstable spiral} \\
\mathsf{Re}\,\lambda_1 < 0 \quad , \ \lambda_2 = \lambda_1^* \quad &: \quad \text{(5) stable spiral}
\end{aligned} \tag{14.38}$$

How many possible generic fixed points are there for an $N = 3$ system?

For a general real $3\times3$ matrix $M$, the characteristic polynomial $P(\lambda) = \det(\lambda - M)$ satisfies $P(\lambda^*) = P(\lambda)$. Thus, if $\lambda$ is a root then so is $\lambda^*$. This means that the eigenvalues are either real or else come in complex conjugate pairs. There are then ten generic possibilities for the three eigenvalues:

$$\begin{aligned}
&(1) && \text{unstable node} && : && \lambda_1 > \lambda_2 > \lambda_3 > 0 \\
&(2) && (++-)\ \text{saddle} && : && \lambda_1 > \lambda_2 > 0 > \lambda_3 \\
&(3) && (+--)\ \text{saddle} && : && \lambda_1 > 0 > \lambda_2 > \lambda_3 \\
&(4) && \text{stable node} && : && 0 > \lambda_1 > \lambda_2 > \lambda_3 \\
&(5) && \text{unstable spiral-node} && : && \lambda_1 > \mathsf{Re}\,\lambda_{2,3} > 0 \ ; \ \mathsf{Im}\,\lambda_2 = -\mathsf{Im}\,\lambda_3 \\
&(6) && \text{unstable spiral-node} && : && \mathsf{Re}\,\lambda_{1,2} > \lambda_3 > 0 \ ; \ \mathsf{Im}\,\lambda_1 = -\mathsf{Im}\,\lambda_2 \\
&(7) && \text{stable spiral-node} && : && 0 > \lambda_1 > \mathsf{Re}\,\lambda_{2,3} \ ; \ \mathsf{Im}\,\lambda_2 = -\mathsf{Im}\,\lambda_3 \\
&(8) && \text{stable spiral-node} && : && 0 > \mathsf{Re}\,\lambda_{1,2} > \lambda_3 \ ; \ \mathsf{Im}\,\lambda_1 = -\mathsf{Im}\,\lambda_2 \\
&(9) && (+--)\ \text{spiral-saddle} && : && \lambda_1 > 0 > \mathsf{Re}\,\lambda_{2,3} \ ; \ \mathsf{Im}\,\lambda_2 = -\mathsf{Im}\,\lambda_3 \\
&(10) && (++-)\ \text{spiral-saddle} && : && \mathsf{Re}\,\lambda_{1,2} > 0 > \lambda_3 \ ; \ \mathsf{Im}\,\lambda_1 = -\mathsf{Im}\,\lambda_2 \quad .
\end{aligned}$$

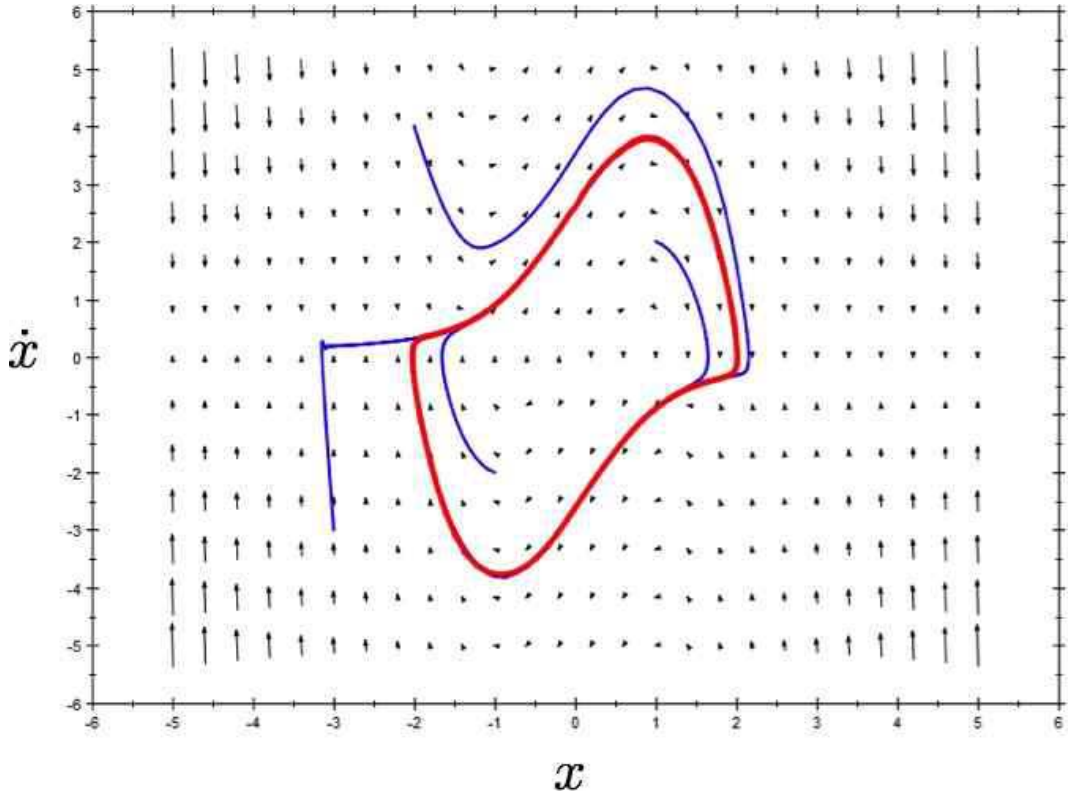


Figure 14.9: Limit cycle of the Van der Pol oscillator for $\mu \gg 1$. (Source: Wikipedia)

## 14.3 Andronov-Hopf Bifurcation

A bifurcation between a spiral and a limit cycle is known as an *Andronov-Hopf bifurcation*. As a simple example, consider the $N = 2$ system,

$$\begin{aligned} \dot{x} &= ax - by - C(x^2 + y^2)\, x \\ \dot{y} &= bx + ay - C(x^2 + y^2)\, y \quad , \end{aligned} \tag{14.39}$$

where $a$, $b$, and $C$ are real. Clearly the origin is a fixed point, at which one finds the eigenvalues $\lambda = a \pm ib$. Thus, the fixed point is a stable spiral if $a < 0$ and an unstable spiral if $a > 0$.

Written in terms of the complex variable $z = x + iy$, these two equations collapse to the single equation

$$\dot{z} = (a + ib)\, z - C\, |z|^2\, z \quad . \tag{14.40}$$

The dynamics are also simple in polar coordinates $r = |z|$, $\theta = \arg(z)$:

$$\begin{aligned} \dot{r} &= ar - Cr^3 \\ \dot{\theta} &= b \quad . \end{aligned} \tag{14.41}$$

The phase diagram, for fixed $b > 0$, is depicted in Fig. 14.10. For positive $a/C$, there is a limit cycle at $r = \sqrt{a/C}$. In both cases, the limit cycle disappears as $a$ crosses the value $a^* = 0$ and is replaced by a stable $(a < 0, C > 0)$ or unstable $(a > 0, C < 0)$ spiral.

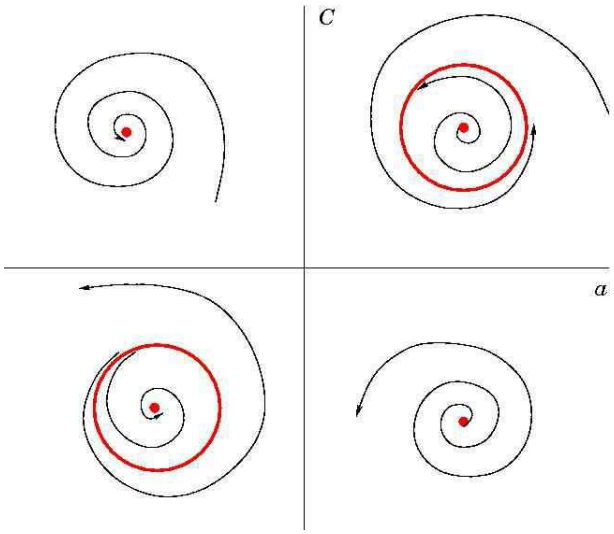


Figure 14.10: Hopf bifurcation: for $C > 0$ the bifurcation is supercritical, between stable spiral and stable limit cycle. For $C < 0$ the bifurcation is subcritical, between unstable spiral and unstable limit cycle. The bifurcation occurs at $a = 0$ in both cases.

This example also underscores the following interesting point. Adding a small nonlinear term $C$ has no fundamental effect on the fixed point behavior so long as $a \neq 0$, when the fixed point is a stable or unstable spiral. In general, fixed points which are attractors (stable spirals or nodes), repellers (unstable spirals or nodes), or saddles are *robust* with respect to the addition of a small nonlinearity. But the fixed point behavior in the marginal cases – centers, stars, degenerate nodes, and fixed lines – is strongly affected by the presence of even a small nonlinearity. In this example, the FP is a center when $a = 0$. But as the $(r, \theta)$ dynamics shows, a small nonlinearity will destroy the center and turn the FP into an attractor $(C > 0)$ or a repeller $(C < 0)$.

## 14.4 Population Biology: Lotka-Volterra Models

Consider two species with populations $N_1$ and $N_2$, respectively[2]. We model the evolution of these populations by the coupled ODEs

$$\begin{aligned} \frac{dN_1}{dt} &= aN_1 + bN_1N_2 + cN_1^2 \\ \frac{dN_2}{dt} &= dN_2 + eN_1N_2 + fN_2^2 \quad , \end{aligned} \tag{14.42}$$

[2]This discussion is adapted from S. Strogatz, *Nonlinear Dynamics and Chaos*.

where $\{a, b, c, d, e, f\}$ are constants. We can eliminate some constants by rescaling $N_{1,2}$. This results in the following:

$$\begin{aligned} \dot{x} &= x\big(r - \mu x - ky\big) \\ \dot{y} &= y\big(r' - \mu' y - k' x\big) \quad , \end{aligned} \tag{14.43}$$

where $\mu$, and $\mu'$ can each take on one of three possible values $\{0, \pm 1\}$. By rescaling time, we can eliminate the scale of either of $r$ or $r'$ as well. Typically, intra-species competition guarantees $\mu = \mu' = +1$. The remaining coefficients $(r, k, k')$ are real may also be of either sign. The values and especially the signs of the various coefficients have a physical (or biological) significance. For example, if $k < 0$ it means that $x$ grows due to the presence of $y$. The effect of $y$ on $x$ may be of the same sign $(kk' > 0)$ or of opposite sign $(kk' < 0)$.

### 14.4.1 Rabbits and foxes

As an example, consider the model

$$\begin{aligned} \dot{x} &= x - xy \\ \dot{y} &= -\beta y + xy \quad . \end{aligned} \tag{14.44}$$

The quantity $x$ might represent the (scaled) population of rabbits and $y$ the population of foxes in an ecosystem. There are two fixed points: at $(0, 0)$ and at $(\beta, 1)$. Linearizing the dynamics about these fixed points, one finds that $(0, 0)$ is a saddle while $(\beta, 1)$ is a center. Let's do this explicitly.

The first step is to find the fixed points $(x^*, y^*)$. To do this, we set $\dot{x} = 0$ and $\dot{y} = 0$. From $\dot{x} = x(1-y) = 0$ we have that $x = 0$ or $y = 1$. Suppose $x = 0$. The second equation, $\dot{y} = (x - \beta)y$ then requires $y = 0$. So $\boldsymbol{P}_1 = (0, 0)$ is a fixed point. The other possibility is that $y = 1$, which then requires $x = \beta$. So $\boldsymbol{P}_2 = (\beta, 1)$ is the second fixed point. Those are the only possibilities.

We now compute the linearized dynamics at these fixed points. The linearized dynamics are given by $\dot{\boldsymbol{\varphi}} = M\boldsymbol{\varphi}$, with

$$M = \begin{pmatrix} \partial\dot{x}/\partial x & \partial\dot{x}/\partial y \\ \partial\dot{y}/\partial x & \partial\dot{y}/\partial y \end{pmatrix} = \begin{pmatrix} 1 - y & -x \\ y & x - \beta \end{pmatrix} \quad . \tag{14.45}$$

Evaluating $M$ at $\boldsymbol{P}_1$ and $\boldsymbol{P}_2$, we find

$$M_1 = \begin{pmatrix} 1 & 0 \\ 0 & -\beta \end{pmatrix} \qquad , \qquad M_2 = \begin{pmatrix} 0 & -\beta \\ 1 & 0 \end{pmatrix} \quad . \tag{14.46}$$

The eigenvalues are easily found:

$$\begin{aligned} \boldsymbol{P}_1 \;:\; \lambda_+ &= 1 \quad , \quad \lambda_- = -\beta \\ \boldsymbol{P}_2 \;:\; \lambda_+ &= i\sqrt{\beta} \quad , \quad \lambda_- = -i\sqrt{\beta} \quad . \end{aligned} \tag{14.47}$$

Thus $\boldsymbol{P}_1$ is a saddle point and $\boldsymbol{P}_2$ is a center.

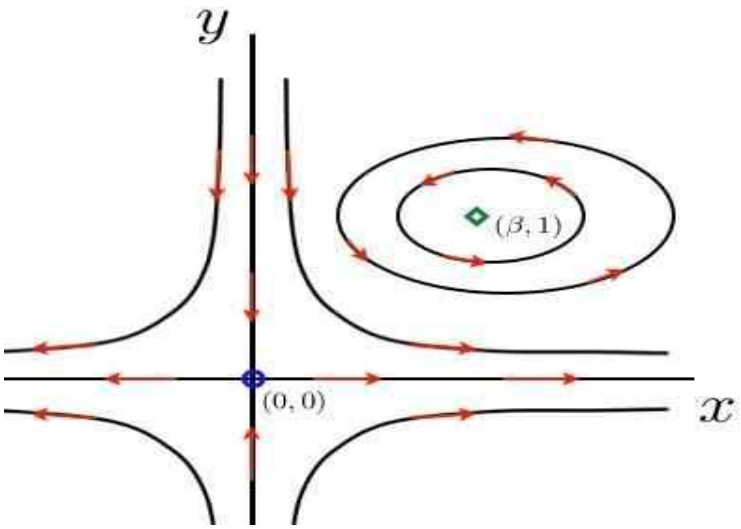


Figure 14.11: Phase flow for the rabbits *vs.* foxes Lotka-Volterra model of eqs. 14.44.

As we saw earlier, generally speaking we expect nonlinear terms to transform centers to stable or unstable spirals, possibly with a limit cycle. However for the Lotka-Volterra system there is a conserved quantity. Consider the general predator-prey system

$$\begin{aligned} \dot{x} &= (a - b\,y)\,x \\ \dot{y} &= -(c - d\,x)\,y \end{aligned} \quad , \tag{14.48}$$

where $a$, $b$, $c$, and $d$ are all positive constants. Now consider the function

$$H \equiv d\,x + b\,y - c\,\log x - a\,\log y \quad . \tag{14.49}$$

Then

$$\frac{\partial H}{\partial x} = d - \frac{c}{x} \qquad , \qquad \frac{\partial H}{\partial y} = b - \frac{a}{y} \quad . \tag{14.50}$$

Thus, we have $\dot{x} = -xy\,\frac{\partial H}{\partial y}$ and $\dot{y} = xy\,\frac{\partial H}{\partial x}$. If we define $p \equiv \log x$ and $q \equiv \log y$, then we have

$$\dot{q} = \frac{\partial H}{\partial p} \qquad , \qquad \dot{p} = -\frac{\partial H}{\partial q} \tag{14.51}$$

with

$$H(q,p) = d\,e^{p} + b\,e^{q} - c\,p - a\,q \quad . \tag{14.52}$$

So the system is a Hamiltonian system in disguise, and we know that for Hamiltonian systems the only possible fixed points are saddles and centers. The phase curves are level sets of the function $H$.

### 14.4.2 Rabbits and sheep

In the rabbits and foxes model of eqs. 14.44, the rabbits are the food for the foxes. This means $k = 1$ but $k' = -1$, *i.e.* the fox population is enhanced by the presence of rabbits, but the rabbit population

is diminished by the presence of foxes. Consider now a model in which the two species (rabbits and sheep, say) compete for food:

$$\begin{aligned} \dot{x} &= x\,(r - x - ky) \\ \dot{y} &= y\,(1 - y - k'x) \end{aligned} \quad , \tag{14.53}$$

with $r$, $k$, and $k'$ all positive. Note that when either population $x$ or $y$ vanishes, the remaining population is governed by the logistic equation, *i.e.* it will flow to a nonzero fixed point.

The matrix of derivatives, which is to be evaluated at each fixed point in order to assess its stability, is

$$M = \begin{pmatrix} \partial\dot{x}/\partial x & \partial\dot{x}/\partial y \\ \partial\dot{y}/\partial x & \partial\dot{y}/\partial y \end{pmatrix} = \begin{pmatrix} r - 2x - ky & -kx \\ -k'y & 1 - 2y - k'x \end{pmatrix} \quad . \tag{14.54}$$

At each fixed point, we must evaluate $D = \mathsf{det}(M)$ and $T = \mathsf{Tr}\,(M)$ and apply the classification scheme of Fig. 14.6.

- $\boldsymbol{P}_1 = (0,0)$ : This is the trivial state with no rabbits ($x = 0$) and no sheep ($y = 0$). The linearized dynamics gives $M_1 = \begin{pmatrix} r & 0 \\ 0 & 1 \end{pmatrix}$, which corresponds to an unstable node.

- $\boldsymbol{P}_2 = (r,0)$ : Here we have rabbits but no sheep. The linearized dynamics gives $M_2 = \begin{pmatrix} -r & -rk \\ 0 & 1 - rk' \end{pmatrix}$. For $rk' > 1$ this is a stable node; for $rk' < 1$ it is a saddle point.

- $\boldsymbol{P}_3 = (0,1)$ : Here we have sheep but no rabbits. The linearized dynamics gives $M_3 = \begin{pmatrix} r - k & 0 \\ -k' & -1 \end{pmatrix}$. For $k > r$ this is a stable node; for $k < r$ it is a saddle.

- There is one remaining fixed point – a nontrivial one where both $x$ and $y$ are nonzero. To find it, we set $\dot{x} = \dot{y} = 0$, and divide out by $x$ and $y$ respectively, to get

$$\begin{aligned} x + ky &= r \\ kx' + y &= 1 \end{aligned} \quad . \tag{14.55}$$

  This is a simple rank 2 inhomogeneous linear system. If the fixed point $\boldsymbol{P}_4$ is to lie in the physical quadrant ($x > 0, y > 0$), then either (i) $k > r$ and $k' > r^{-1}$ or (ii) $k < r$ and $k' < r^{-1}$. The solution is

$$\boldsymbol{P}_4 = \begin{pmatrix} 1 & k \\ k' & 1 \end{pmatrix}^{-1} \begin{pmatrix} r \\ 1 \end{pmatrix} = \frac{1}{1 - kk'} \begin{pmatrix} r - k \\ 1 - rk' \end{pmatrix} \quad . \tag{14.56}$$

  The linearized dynamics then gives

$$M_4 = \frac{1}{1 - kk'} \begin{pmatrix} k - r & k(k - r) \\ k'(rk' - 1) & rk' - 1 \end{pmatrix} \quad , \tag{14.57}$$

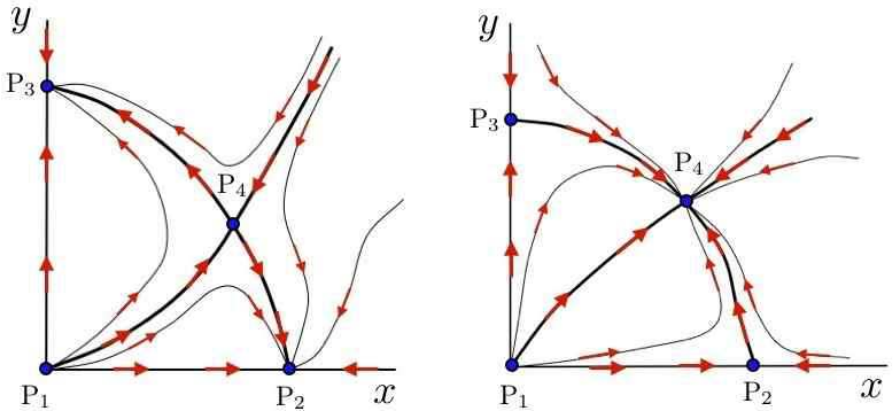


Figure 14.12: Two possible phase flows for the rabbits *vs.* sheep model of eqs. 14.53. Left panel: $k > r > k'^{-1}$. Right panel: $k < r < k'^{-1}$.

yielding

$$T = \frac{rk' - 1 + k - r}{1 - kk'}$$
$$D = \frac{(k - r)(rk' - 1)}{1 - kk'} \quad . \tag{14.58}$$

The classification of this fixed point can vary with parameters. Consider the case $r = 1$. If $k = k' = 2$ then both $\boldsymbol{P}_2$ and $\boldsymbol{P}_3$ are stable nodes. At $\boldsymbol{P}_4$, one finds $T = -\frac{2}{3}$ and $D = -\frac{1}{3}$, corresponding to a saddle point. In this case it is the fate of one population to die out at the expense of the other, and which one survives depends on initial conditions. If instead we took $k = k' = \frac{1}{2}$, then $T = -\frac{4}{3}$ and $D = \frac{1}{3}$, corresponding to a stable node (node $D < \frac{1}{4}T^2$ in this case). The situation is depicted in Fig. 14.12.

## 14.5 Poincaré-Bendixson Theorem

Although $N = 2$ systems are much richer than $N = 1$ systems, they are still ultimately rather impoverished in terms of their long-time behavior. If an orbit does not flow off to infinity or asymptotically approach a stable fixed point (node or spiral or nongeneric example), the only remaining possibility is limit cycle behavior. This is the content of the *Poincaré-Bendixson theorem*, which states:

- *IF* $\Omega$ is a compact (*i.e.* closed and bounded) subset of phase space,
- *AND* $\dot{\boldsymbol{\varphi}} = \boldsymbol{V}(\boldsymbol{\varphi})$ is continuously differentiable on $\Omega$,
- *AND* $\Omega$ contains no fixed points (*i.e.* $\boldsymbol{V}(\boldsymbol{\varphi})$ never vanishes in $\Omega$),
- *AND* a phase curve $\boldsymbol{\varphi}(t)$ is always confined to $\Omega$,
- $\diamond$ *THEN* $\boldsymbol{\varphi}(t)$ is either closed or approaches a closed trajectory in the limit $t \to \infty$.

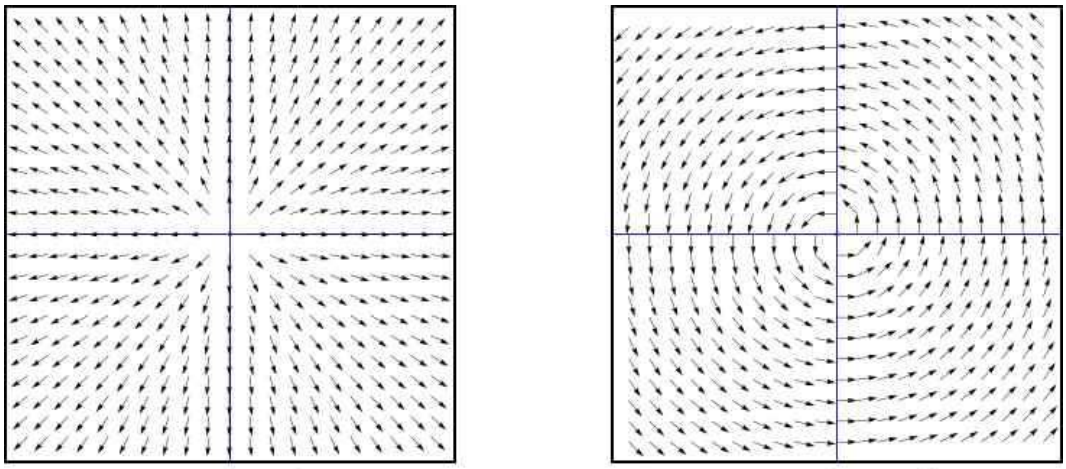


Figure 14.13: Two singularities with index $+1$. The direction field $\widehat{\boldsymbol{V}} = \boldsymbol{V}/\big|\boldsymbol{V}\big|$ is shown in both cases.

Thus, under the conditions of the theorem, $\Omega$ must contain a closed orbit.

One way to prove that $\boldsymbol{\varphi}(t)$ is confined to $\Omega$ is to establish that $\boldsymbol{V}\cdot\hat{\boldsymbol{n}} \leq 0$ everywhere on the boundary $\partial\Omega$, which means that the phase flow is always directed inward (or tangent) along the boundary. Let's analyze an example from the book by Strogatz. Consider the system

$$\begin{aligned}\dot r &= r(1-r^2) + \lambda\, r\,\cos\theta \\ \dot\theta &= 1 \quad ,\end{aligned} \tag{14.59}$$

with $0 < \lambda < 1$. Then define

$$a \equiv \sqrt{1-\lambda} \quad , \quad b \equiv \sqrt{1+\lambda} \tag{14.60}$$

and

$$\Omega \equiv \Big\{ (r,\theta) \;\Big|\; a < r < b \Big\} \quad . \tag{14.61}$$

On the boundaries of $\Omega$, we have

$$\begin{aligned} r = a \qquad &\Rightarrow \qquad \dot r = \lambda\, a\,\big(1+\cos\theta\big) \\ r = b \qquad &\Rightarrow \qquad \dot r = -\lambda\, b\,\big(1-\cos\theta\big) \quad .\end{aligned} \tag{14.62}$$

We see that the radial component of the flow is inward along both $r = a$ and $r = b$. Thus, any trajectory which starts inside $\Omega$ can never escape. The Poincaré-Bendixson theorem tells us that the trajectory will approach a stable limit cycle in the limit $t \to \infty$.

It is only with $N \geq 3$ systems that the interesting possibility of chaotic behavior emerges.

## 14.6 Index Theory

Consider a smooth two-dimensional vector field $\boldsymbol{V}(\boldsymbol{\varphi})$. The angle that the vector $\boldsymbol{V}$ makes with respect to the $\widehat{\boldsymbol{\varphi}}_1$ and $\widehat{\boldsymbol{\varphi}}_2$ axes is a scalar field,

$$\Theta(\boldsymbol{\varphi}) = \tan^{-1}\left(\frac{V_2(\boldsymbol{\varphi})}{V_1(\boldsymbol{\varphi})}\right) \quad . \tag{14.63}$$

So long as $\boldsymbol{V}$ has finite length, the angle $\Theta$ is well-defined. In particular, we expect that we can integrate $\boldsymbol{\nabla}\Theta$ over a closed curve $\mathcal{C}$ in phase space to get

$$\oint\limits_{\mathcal{C}} d\boldsymbol{\varphi}\cdot\boldsymbol{\nabla}\Theta = 0 \quad . \tag{14.64}$$

However, this can fail if $\boldsymbol{V}(\boldsymbol{\varphi})$ vanishes (or diverges) at one or more points in the interior of $\mathcal{C}$. In general, if we define

$$\mathsf{W}_{\mathcal{C}}(\boldsymbol{V}) = \frac{1}{2\pi}\oint\limits_{\mathcal{C}} d\boldsymbol{\varphi}\cdot\boldsymbol{\nabla}\Theta \quad , \tag{14.65}$$

then $\mathsf{W}_{\mathcal{C}}(\boldsymbol{V}) \in \mathbb{Z}$ is an integer valued function of $\mathcal{C}$, which is the change in $\Theta$ around the curve $\mathcal{C}$. This must be an integer, because $\Theta$ is well-defined only up to multiples of $2\pi$. Note that *differential changes* of $\Theta$ are in general well-defined.

Thus, if $\boldsymbol{V}(\boldsymbol{\varphi})$ is finite, meaning neither infinite nor infinitesimal, *i.e.* $\boldsymbol{V}$ neither diverges nor vanishes anywhere in $\mathrm{int}(\mathcal{C})$, then $\mathsf{W}_{\mathcal{C}}(\boldsymbol{V}) = 0$. Assuming that $\boldsymbol{V}$ never diverges, any singularities in $\Theta$ must arise from points where $\boldsymbol{V} = 0$, which in general occurs at isolated points, since it entails two equations in the two variables $(\varphi_1\,,\,\varphi_2)$.

The index of a two-dimensional vector field $\boldsymbol{V}(\boldsymbol{\varphi})$ at a *point* $\boldsymbol{\varphi}$ is the integer-valued winding of $\boldsymbol{V}$ about that point:

$$\begin{aligned}\mathop{\mathsf{ind}}_{\boldsymbol{\varphi}_0}(\boldsymbol{V}) &= \lim_{a\to 0}\,\frac{1}{2\pi}\oint\limits_{\mathcal{C}_a(\boldsymbol{\varphi}_0)} d\boldsymbol{\varphi}\cdot\boldsymbol{\nabla}\Theta \\ &= \lim_{a\to 0}\,\frac{1}{2\pi}\oint\limits_{\mathcal{C}_a(\boldsymbol{\varphi}_0)} d\boldsymbol{\varphi}\cdot\frac{V_1\boldsymbol{\nabla}V_2 - V_2\boldsymbol{\nabla}V_1}{V_1^2+V_2^2} \quad ,\end{aligned} \tag{14.66}$$

where $\mathcal{C}_a(\boldsymbol{\varphi}_0)$ is a circle of radius $a$ surrounding the point $\boldsymbol{\varphi}_0$. The index of a closed curve $\mathcal{C}$ is given by the sum of the indices at all the singularities enclosed by the curve:[3]

$$\mathsf{W}_{\mathcal{C}}(\boldsymbol{V}) = \sum_{\boldsymbol{\varphi}_i\,\in\,\mathrm{int}(\mathcal{C})}\mathop{\mathsf{ind}}_{\boldsymbol{\varphi}_i}(\boldsymbol{V}) \quad . \tag{14.67}$$

[3]Technically, we should weight the index at each enclosed singularity by the signed number of times the curve $\mathcal{C}$ encloses that singularity. For simplicity and clarity, we assume that the curve $\mathcal{C}$ is homeomorphic to the circle $\mathbb{S}^1$.

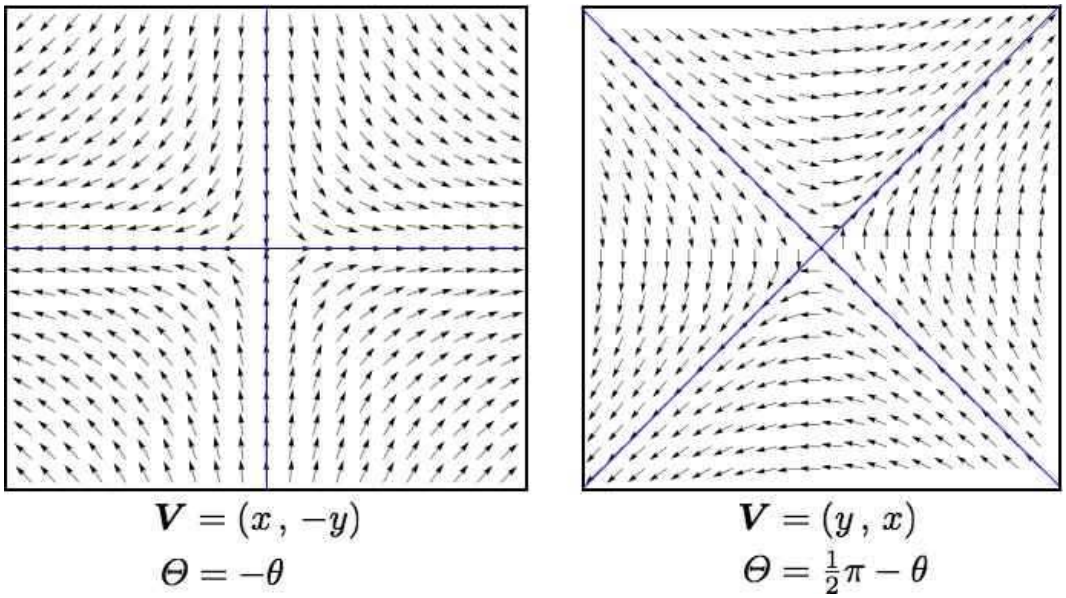


Figure 14.14: Two singularities with index $-1$.

As an example, consider the vector fields plotted in fig. 14.13. We have:

$$\begin{aligned} \boldsymbol{V} &= (x\,,\,y) \quad \Rightarrow \quad \Theta = \theta \\ \boldsymbol{V} &= (-y\,,\,x) \quad \Rightarrow \quad \Theta = \theta + \tfrac{1}{2}\pi \quad . \end{aligned} \tag{14.68}$$

The index is the same, $+1$, in both cases, even though the first corresponds to an unstable node and the second to a center. Any $N = 2$ fixed point with $\det M > 0$ has index $+1$.

Fig. 14.14 shows two vector fields, each with index $-1$:

$$\begin{aligned} \boldsymbol{V} &= (x\,,\,-y) \quad \Rightarrow \quad \Theta = -\theta \\ \boldsymbol{V} &= (y\,,\,x) \quad \Rightarrow \quad \Theta = -\theta + \tfrac{1}{2}\pi \quad . \end{aligned} \tag{14.69}$$

In both cases, the fixed point is a saddle.

As an example of the content of eqn. 14.67, consider the vector fields in eqn. 14.15. The left panel shows the vector field $\boldsymbol{V} = (x^2 - y^2\,,\,2xy)$, which has a single fixed point, at the origin $(0\,,\,0)$, of index $+2$. The right panel shows the vector field $\boldsymbol{V} = (1 + x^2 - y^2\,,\,x + 2xy)$, which has fixed points $(x^*\,,\,y^*)$ at $(0\,,\,1)$ and $(0\,,\,-1)$. The linearized dynamics is given by the matrix

$$M = \begin{pmatrix} \frac{\partial \dot{x}}{\partial x} & \frac{\partial \dot{x}}{\partial y} \\ \frac{\partial \dot{y}}{\partial x} & \frac{\partial \dot{y}}{\partial y} \end{pmatrix} = \begin{pmatrix} 2x & -2y \\ 1+2y & 2x \end{pmatrix} \quad . \tag{14.70}$$

Thus,

$$M_{(0,1)} = \begin{pmatrix} 0 & -2 \\ 2 & 0 \end{pmatrix} \quad , \quad M_{(0,-1)} = \begin{pmatrix} 0 & 2 \\ -2 & 0 \end{pmatrix} \quad . \tag{14.71}$$

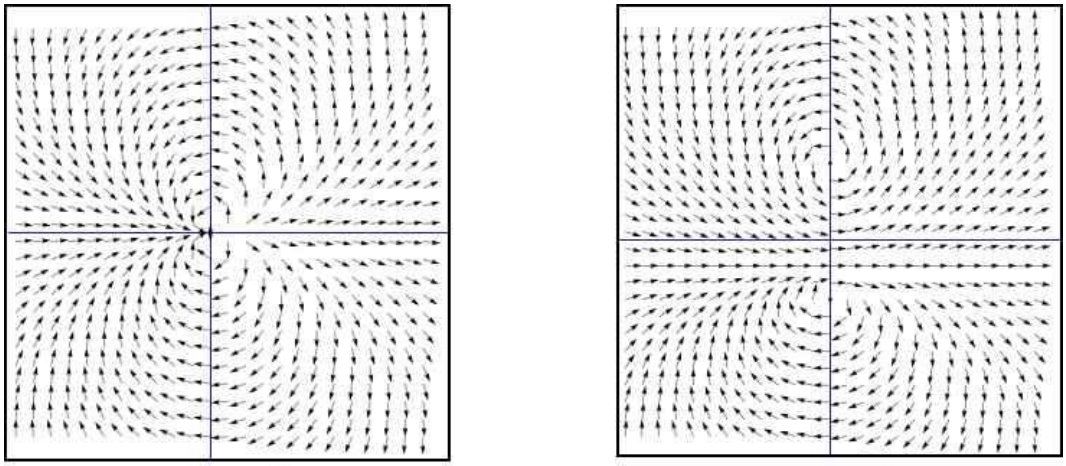


Figure 14.15: Left panel: a singularity with index $+2$. Right panel: two singularities each with index $+1$. Note that the long distance behavior of $\boldsymbol{V}$ is the same in both cases.

At each of these fixed points, we have $T = 0$ and $D = 4$, corresponding to a center, with index $+1$. If we consider a square-ish curve $\mathcal{C}$around the periphery of each figure, the vector field is almost the same along such a curve for both the left and right panels, and the winding number is $\mathsf{W}_{\mathcal{C}}(\boldsymbol{V}) = +2$.

Finally, consider the vector field shown in fig. 14.16, with $\boldsymbol{V} = (x^2 - y^2\,,\, -2xy)$. Clearly $\Theta = -2\theta$, and the index of the singularity at $(0\,,\,0)$ is $-2$.

To recapitulate some properties of the index / winding number:

- The index $\mathsf{ind}_{\boldsymbol{\varphi}_0}(\boldsymbol{V})$ of an $N = 2$ vector field $\boldsymbol{V}$ at a point $\boldsymbol{\varphi}_0$ is the winding number of $\boldsymbol{V}$ about that point.
- The winding number $\mathsf{W}_{\mathcal{C}}(\boldsymbol{V})$ of a curve $\mathcal{C}$ is the sum of the indices of the singularities enclosed by that curve.
- Smooth deformations of $\mathcal{C}$ do not change its winding number. One must instead "stretch" $\mathcal{C}$ over a fixed point singularity in order to change $\mathsf{W}_{\mathcal{C}}(\boldsymbol{V})$.
- Uniformly rotating each vector in the vector field by an angle $\beta$ has the effect of sending $\Theta \to \Theta + \beta$; this leaves all indices and winding numbers invariant.
- Nodes and spirals, whether stable or unstable, have index $+1$ (ss do the special cases of centers, stars, and degenerate nodes). Saddle points have index $-1$.
- Clearly any closed orbit must lie on a curve $\mathcal{C}$ of index $+1$.

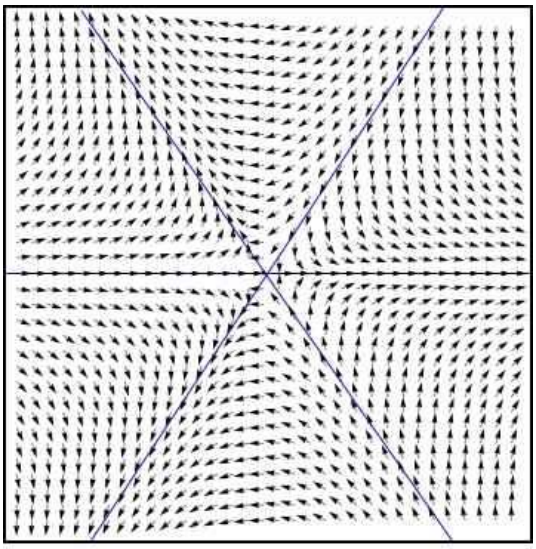


Figure 14.16: A vector field with index $-2$.

### 14.6.1 Gauss-Bonnet theorem

There is a deep result in mathematics, the Gauss-Bonnet theorem, which connects the local *geometry* of a two-dimensional manifold to its global *topological structure*. The content of the theorem is as follows:

$$\int_{\mathcal{M}} dA\, K = 2\pi\, \chi(\mathcal{M}) = 2\pi \sum_i \mathsf{ind}_{\boldsymbol{\varphi}_i}(\boldsymbol{V}) \quad , \tag{14.72}$$

where $\mathcal{M}$ is a 2-manifold (a topological space locally homeomorphic to $\mathbb{R}^2$), $\kappa$ is the local *Gaussian curvature* of $\mathcal{M}$, which is given by $K = (R_1\, R_2)^{-1}$, where $R_{1,2}$ are the principal radii of curvature at a given point, and $dA$ is the differential area element. The quantity $\chi(\mathcal{M})$ is called the *Euler characteristic* of $\mathcal{M}$ and is given by $\chi(\mathcal{M}) = 2 - 2g$, where $g$ is the *genus* of $\mathcal{M}$, which is the number of holes (or handles) of $\mathcal{M}$. Furthermore, $\boldsymbol{V}(\boldsymbol{\varphi})$ is *any* smooth vector field on $\mathcal{M}$, and $\boldsymbol{\varphi}_i$ are the singularity points of that vector field, which are fixed points of the dynamics $\dot{\boldsymbol{\varphi}} = \boldsymbol{V}(\boldsymbol{\varphi})$.

To apprehend the content of the Gauss-Bonnet theorem, it is helpful to consider an example. Let $\mathcal{M} = \mathbb{S}^2$ be the unit 2-sphere, as depicted in fig. 14.17. At any point on the unit 2-sphere, the radii of curvature are degenerate and both equal to $R = 1$, hence $K = 1$. If we integrate the Gaussian curvature over the sphere, we thus get $4\pi = 2\pi\,\chi(\mathbb{S}^2)$, which says $\chi(\mathbb{S}^2) = 2 - 2g = 2$, which agrees with $g = 0$ for the sphere. Furthermore, the Gauss-Bonnet theorem says that *any* smooth vector field on $\mathbb{S}^2$ *must* have a singularity or singularities, with the total index summed over the singularities equal to $+2$. The vector field sketched in the left panel of fig. 14.17 has two index $+1$ singularities, which could be taken at the north and south poles, but which could be anywhere. Another possibility, depicted in the right panel of fig. 14.17, is that there is a one singularity with index $+2$.

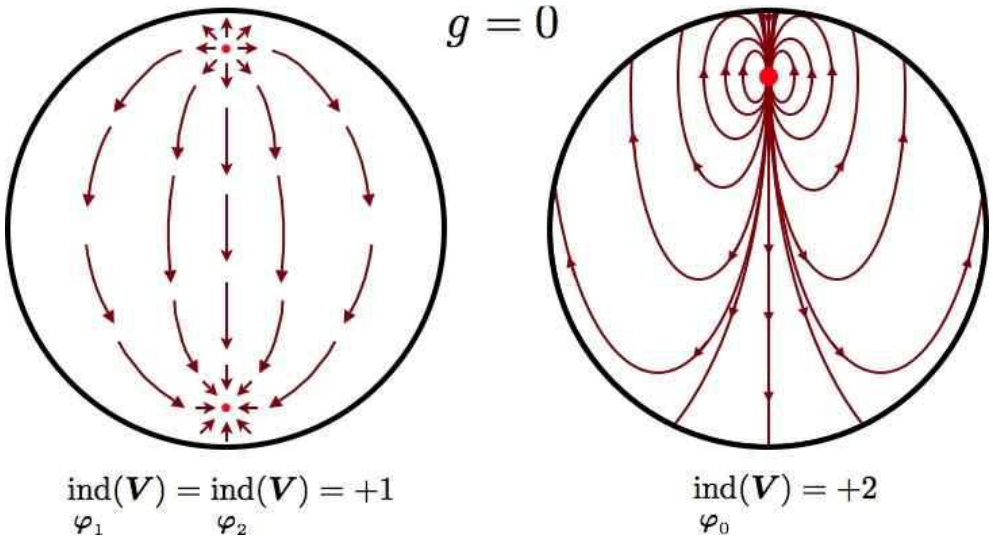


Figure 14.17: Two smooth vector fields on the sphere $\mathbb{S}^2$, which has genus $g = 0$. Left panel: two index $+1$ singularities. Right panel: one index $+2$ singularity.

In fig. 14.18 we show examples of manifolds with genii $g = 1$ and $g = 2$. The case $g = 1$ is the familiar 2-torus, which is topologically equivalent to a product of circles: $\mathbb{T}^2 \simeq \mathbb{S}^1 \times \mathbb{S}^1$, and is thus coordinatized by two angles $\theta_1$ and $\theta_2$. A smooth vector field pointing in the direction of increasing $\theta_1$ never vanishes, and thus has no singularities, consistent with $g = 1$ and $\chi\big(\mathbb{T}^2\big) = 0$. Topologically, one can define a torus as the quotient space $\mathbb{R}^2/\mathbb{Z}^2$, or as a square with opposite sides identified. This is what mathematicians call a 'flat torus' – one with curvature $K = 0$ everywhere. Of course, such a torus cannot be embedded in three-dimensional Euclidean space; a two-dimensional figure embedded in a three-dimensional Euclidean space inherits a metric due to the embedding, and for a physical torus, like the surface of a bagel, the Gaussian curvature is only zero *on average*.

The $g = 2$ surface $\mathcal{M}$ shown in the right panel of fig. 14.18 has Euler characteristic $\chi(\mathcal{M}) = -2$, which means that any smooth vector field on $\mathcal{M}$ must have singularities with indices totalling $-2$. One possibility, depicted in the figure, is to have two saddle points with index $-1$; one of these singularities is shown in the figure (the other would be on the opposite side).

### 14.6.2 Singularities and topology

For any $N = 1$ system $\dot{x} = f(x)$, we can identify a 'charge' $Q$ with any generic fixed point $x^*$ by setting

$$Q = \mathsf{sgn}\Big[f'(x^*)\Big] \quad , \tag{14.73}$$

where $f(x^*) = 0$. The total charge contained in a region $\big[x_1, x_2\big]$ is then

$$Q_{12} = \tfrac{1}{2}\,\mathsf{sgn}\Big[f(x_2)\Big] - \tfrac{1}{2}\,\mathsf{sgn}\Big[f(x_1)\Big] \quad . \tag{14.74}$$

It is easy to see that $Q_{12}$ is the sum of the charges of all the fixed points lying within the interval $\big[x_1, x_2\big]$.

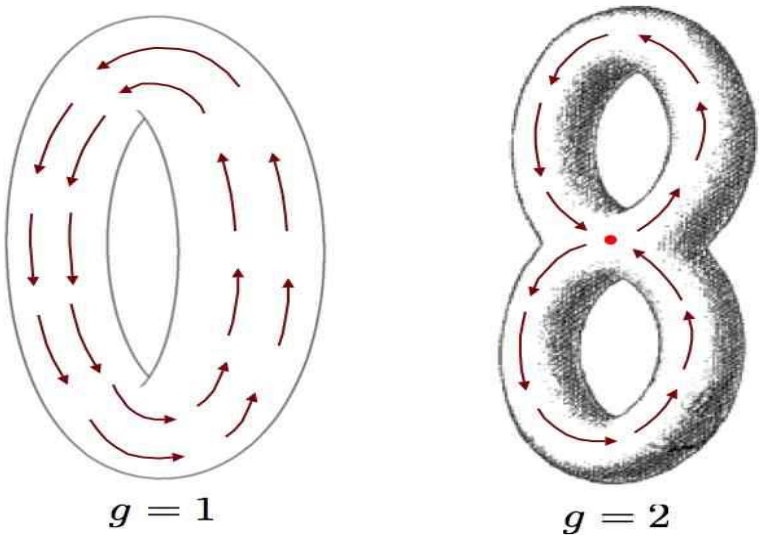


Figure 14.18: Smooth vector fields on the torus $\mathbb{T}^2$ ($g = 1$), and on a 2-manifold $\mathcal{M}$ of genus $g = 2$.

In higher dimensions, we have the following general construction. Consider an $N$-dimensional dynamical system $\dot{\boldsymbol{x}} = \boldsymbol{V}(\boldsymbol{x})$, and let $\hat{\boldsymbol{n}}(\boldsymbol{x})$ be the unit vector field defined by

$$\hat{\boldsymbol{n}}(\boldsymbol{x}) = \frac{\boldsymbol{V}(\boldsymbol{x})}{|\boldsymbol{V}(\boldsymbol{x})|} \quad . \tag{14.75}$$

Consider now a unit sphere in $\hat{\boldsymbol{n}}$ space, which is of dimension $(N-1)$. If we integrate over this surface, we obtain

$$\Omega_N = \oint d\sigma_a \, n^a = \frac{2\pi^{(N-1)/2}}{\Gamma\left(\frac{N-1}{2}\right)} \quad , \tag{14.76}$$

which is the surface area of the unit sphere $\mathbb{S}^{N-1}$. Thus, $\Omega_2 = 2\pi$, $\Omega_3 = 4\pi$, $\Omega_4 = 2\pi^2$, *etc.*

Now consider a change of variables over the surface of the sphere, to the set $(\xi_1, \ldots, \xi_{N-1})$. We then have

$$\Omega_N = \oint\limits_{\mathbb{S}^{N-1}} d\sigma_a \, n^a = \oint d^{N-1}\xi \, \epsilon_{a_1 \cdots a_N} \, n^{a_1} \, \frac{\partial n^{a_2}}{\partial \xi_1} \cdots \frac{\partial n^{a_N}}{\partial \xi_{N-1}} \tag{14.77}$$

The topological charge is then

$$Q = \frac{1}{\Omega_N} \oint d^{N-1}\xi \, \epsilon_{a_1 \cdots a_N} \, n^{a_1} \, \frac{\partial n^{a_2}}{\partial \xi_1} \cdots \frac{\partial n^{a_N}}{\partial \xi_{N-1}} \tag{14.78}$$

The quantity $Q$ is an *integer topological invariant* which characterizes the map from the surface $(\xi_1, \ldots, \xi_{N-1})$ to the unit sphere $|\hat{\boldsymbol{n}}| = 1$. In mathematical parlance, $Q$ is known as the *Pontrjagin index* of this map.

This analytical development recapitulates some basic topology. Let $\mathcal{M}$ be a topological space and consider a map from the circle $\mathbb{S}^1$ to $\mathcal{M}$. We can compose two such maps by merging the two circles, as shown in fig. 14.19. Two maps are said to be *homotopic* if they can be smoothly deformed into each other. Any two homotopic maps are said to belong to the same *equivalence class* or *homotopy class*. For general

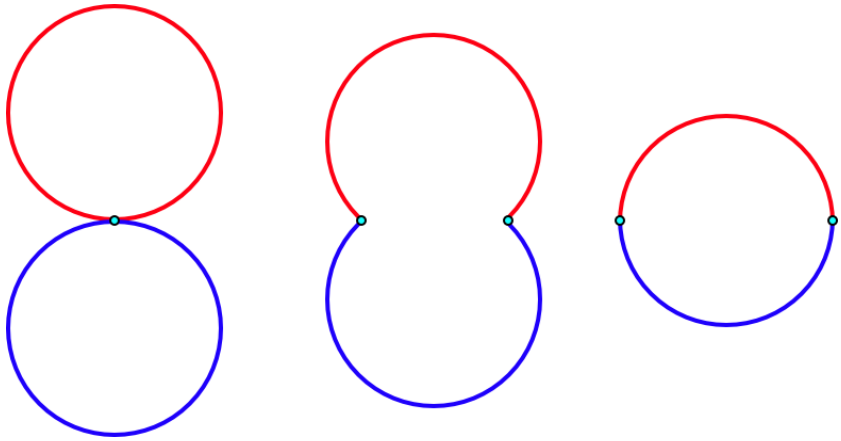

Figure 14.19: Composition of two circles. The same general construction applies to the merging of $n$-spheres $\mathbb{S}^n$, called the *wedge sum*.

$\mathcal{M}$, the homotopy classes may be multiplied using the composition law, resulting in a group structure. The group is called the *fundamental group* of the manifold $\mathcal{M}$, and is abbreviated $\pi_1(\mathcal{M})$. If $\mathcal{M} = \mathbb{S}^2$, then any such map can be smoothly contracted to a point on the 2-sphere, which is to say a trivial map. We then have $\pi_1(\mathcal{M}) = 0$. If $\mathcal{M} = \mathbb{S}^1$, the maps can wind nontrivially, and the homotopy classes are labeled by a single integer winding number: $\pi_1(\mathbb{S}^1) = \mathbb{Z}$. The winding number of the composition of two such maps is the sum of their individual winding numbers. If $\mathcal{M} = \mathbb{T}^2$, the maps can wind nontrivially around either of the two cycles of the 2-torus. We then have $\pi_1(\mathbb{T}^2) = \mathbb{Z}^2$, and in general $\pi_1(\mathbb{T}^n) = \mathbb{Z}^n$. This makes good sense, since an $n$-torus is topologically equivalent to a product of $n$ circles. In some cases, $\pi_1(\mathcal{M})$ can be nonabelian, as is the case when $\mathcal{M}$ is the genus $g = 2$ structure shown in the right hand panel of fig. 14.18.

In general we define the $n^{\rm th}$ *homotopy group* $\pi_n(\mathcal{M})$ as the group under composition of maps from $\mathbb{S}^n$ to $\mathcal{M}$. For $n \geq 2$, $\pi_n(\mathcal{M})$ is abelian. If $\dim(\mathcal{M}) < n$, then $\pi_n(\mathcal{M}) = 0$. In general, $\pi_n(\mathbb{S}^n) = \mathbb{Z}$. These $n^{\rm th}$ homotopy classes of the $n$-sphere are labeled by their Pontrjagin index $Q$.

Finally, we ask what is $Q$ in terms of the eigenvalues and eigenvectors of the linearized map

$$M_{ij} = \left.\frac{\partial V_i}{\partial x_j}\right|_{\boldsymbol{x}^*} \quad . \tag{14.79}$$

For simple cases where all the $\lambda_i$ are nonzero, we have

$$Q = \mathsf{sgn}\left(\prod_{i=1}^{N} \lambda_i\right) \quad . \tag{14.80}$$

## 14.7 Appendix: Example Problem

Consider the two-dimensional phase flow,

$$\begin{aligned} \dot{x} &= \tfrac{1}{2}x + xy - 2x^3 \\ \dot{y} &= \tfrac{5}{2}y + xy - y^2 \end{aligned} \quad . \tag{14.81}$$

(a) Find and classify all fixed points.

Solution : We have

$$\begin{aligned} \dot{x} &= x\left(\tfrac{1}{2} + y - 2x^2\right) \\ \dot{y} &= y\left(\tfrac{5}{2} + x - y\right) \end{aligned} \quad . \tag{14.82}$$

The matrix of first derivatives is

$$M = \begin{pmatrix} \frac{\partial \dot{x}}{\partial x} & \frac{\partial \dot{x}}{\partial y} \\ \\ \frac{\partial \dot{y}}{\partial x} & \frac{\partial \dot{y}}{\partial y} \end{pmatrix} = \begin{pmatrix} \frac{1}{2} + y - 6x^2 & x \\ \\ y & \frac{5}{2} + x - 2y \end{pmatrix} \quad . \tag{14.83}$$

There are six fixed points.

$(x, y) = (0, 0)$ : The derivative matrix is

$$M = \begin{pmatrix} \frac{1}{2} & 0 \\ 0 & \frac{5}{2} \end{pmatrix} \quad . \tag{14.84}$$

The determinant is $D = \frac{5}{4}$ and the trace is $T = 3$. Since $D < \frac{1}{4}T^2$ and $T > 0$, this is an unstable node. (Duh! One can read off both eigenvalues are real and positive.) Eigenvalues: $\lambda_1 = \frac{1}{2}$, $\lambda_2 = \frac{5}{2}$.

$(x, y) = (0, \frac{5}{2})$ : The derivative matrix is

$$M = \begin{pmatrix} 3 & 0 \\ \frac{5}{2} & -\frac{5}{2} \end{pmatrix} \quad , \tag{14.85}$$

for which $D = -\frac{15}{2}$ and $T = \frac{1}{2}$. The determinant is negative, so this is a saddle. Eigenvalues: $\lambda_1 = -\frac{5}{2}$, $\lambda_2 = 3$.

$(x, y) = (-\frac{1}{2}, 0)$ : The derivative matrix is

$$M = \begin{pmatrix} -1 & -\frac{1}{2} \\ 0 & 2 \end{pmatrix} \quad , \tag{14.86}$$

for which $D = -2$ and $T = +1$. The determinant is negative, so this is a saddle. Eigenvalues: $\lambda_1 = -1$, $\lambda_2 = 2$.

$(x, y) = (\frac{1}{2}, 0)$ : The derivative matrix is

$$M = \begin{pmatrix} -1 & \frac{1}{2} \\ 0 & 3 \end{pmatrix} \quad , \tag{14.87}$$

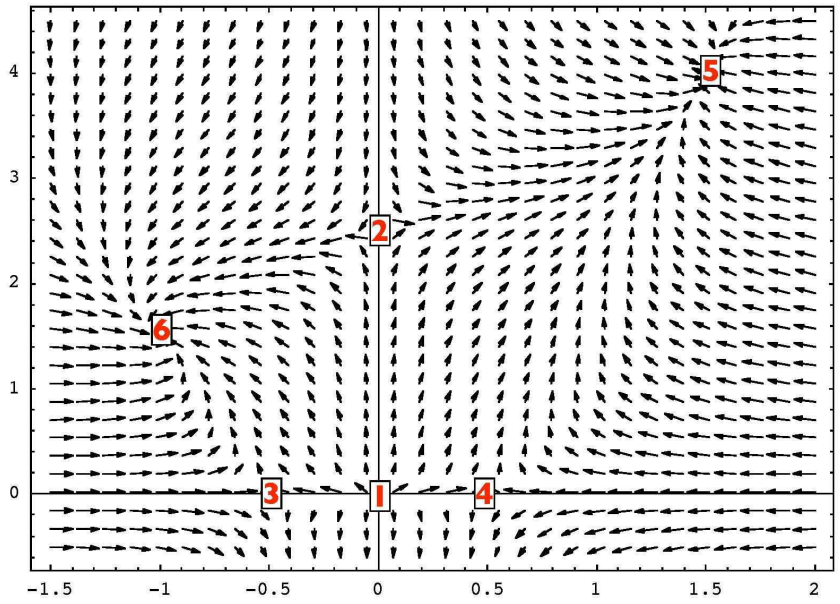


Figure 14.20: Sketch of phase flow for $\dot{x} = \frac{1}{2}x + xy - 2x^3$, $\dot{y} = \frac{5}{2}y + xy - y^2$. Fixed point classifications are in the text.

for which $D = -3$ and $T = +2$. The determinant is negative, so this is a saddle. Eigenvalues: $\lambda_1 = -1$, $\lambda_2 = 3$.

$(x, y) = (\frac{3}{2}, 4)$ : This is one root obtained by setting $y = x + \frac{5}{2}$ and the solving $\frac{1}{2} + y - 2x^2 = 3 + x - 2x^2 = 0$, giving $x = -1$ and $x = +\frac{3}{2}$. The derivative matrix is

$$M = \begin{pmatrix} -9 & \frac{3}{2} \\ 4 & -4 \end{pmatrix} \quad , \tag{14.88}$$

for which $D = 30$ and $T = -13$. Since $D < \frac{1}{4}T^2$ and $T < 0$, this corresponds to a stable node. Eigenvalues: $\lambda_1 = -10$, $\lambda_2 = -3$.

$(x, y) = (-1, \frac{3}{2})$ : This is the second root obtained by setting $y = x + \frac{5}{2}$ and the solving $\frac{1}{2} + y - 2x^2 = 3 + x - 2x^2 = 0$, giving $x = -1$ and $x = +\frac{3}{2}$. The derivative matrix is

$$M = \begin{pmatrix} -4 & -1 \\ \frac{3}{2} & -\frac{3}{2} \end{pmatrix} \quad , \tag{14.89}$$

for which $D = \frac{15}{2}$ and $T = -\frac{11}{2}$. Since $D < \frac{1}{4}T^2$ and $T < 0$, this corresponds to a stable node. Eigenvalues: $\lambda_1 = -3$, $\lambda_2 = -\frac{5}{2}$.

(b) Sketch the phase flow.

Solution : The flow is sketched in fig. 14.20. Thanks to Evan Bierman for providing the Mathematica code.